Published in final edited form as:
Mol Cell Endocrinol. 2010 April 12; 317(1-2): 112. doi:10.1016/j.mce.2009.12.025.

The Müllerian *HOXA10* gene promotes growth of ovarian surface epithelial cells by stimulating epithelial-stromal interactions

Song Yi Ko[1,2], **Ernst Lengyel**[3], and **Honami Naora**[1,2]

[1] Department of Systems Biology, University of Texas M.D. Anderson Cancer Center, Houston, TX

[2] Cancer Biology Program, Graduate School of Biomedical Sciences, University of Texas Health Sciences Center, Houston, TX

[3] Department of Obstetrics and Gynecology/Section of Gynecologic Oncology University of Chicago, Chicago, IL

Summary

The ovarian surface epithelium (OSE) origin of ovarian cancers has been controversial because these cancers often exhibit Müllerian-like features. One hypothesis is that ovarian neoplasia involves the gain of growth advantages by OSE cells via activation of Müllerian programs. The homeobox gene *HOXA10* controls formation of the uterus from the Müllerian ducts, and is not expressed in normal OSE. We previously found that *HOXA10* is expressed in ovarian cancers with endometrial-like features, and induces transformed OSE cells to form glandular tumors in mice. In the current study, we found that induction of *HOXA10* in OSE cells promotes homophilic cell adhesion and prevents anoikis. *HOXA10* expression stimulated interactions of OSE cells with the extracellular matrix proteins vitronectin and fibronectin, and with mesothelial cells of the omentum which is a common attachment site for ovarian cancer cells. *HOXA10* also stimulated interactions of OSE cells with omental fibroblasts, and these interactions promoted OSE cell growth. Our findings indicate that aberrant activation of a Müllerian program in OSE cells confers growth advantages by stimulating cellular interactions with the microenvironment.

Keywords

ovarian surface epithelium; homeobox gene; epithelial-stromal interaction

1. Introduction

The ovarian surface epithelium (OSE) and the Müllerian ducts, which differentiate to form the female reproductive tract, derive from the embryonic coelomic epithelium (Auersperg et al., 2001; Guioli et al., 2007). The OSE is a simple monolayer that resembles the mesothelial lining of the abdominal cavity, whereas Müllerian epithelium is organized in tubal or glandular structures. Many epithelial ovarian cancers exhibit morphologic features that resemble those of the Müllerian lineages. Endometrioid ovarian tumors are characterized by endometrial-like

Corresponding Author: Honami Naora, Ph.D. University of Texas M.D. Anderson Cancer Center Department of Systems Biology 7435 Fannin Street – Unit 950 Houston, TX 77054, U.S.A. Tel: 713-563-4222 Fax: 713-563-4235 hnaora@mdanderson.org.

glandular structures. Serous ovarian tumors resemble cancers of the fallopian tube, whereas mucinous ovarian tumors are composed of endocervical- or intestinal- like cells (Feeley and Wells, 2001; Naora, 2007). The lack of explanation for the Müllerian-like features of ovarian cancers has prompted considerable debate challenging the traditional notion that the OSE is the cell-of-origin of these cancers (Dubeau, 2008; Lee et al., 2007). On the other hand, the OSE origin has been supported by several mouse genetic models of ovarian cancer (Connolly et al., 2003; Fleshken-Nikitin et al., 2003; Orsulic et al., 2002; Wu et al., 2007). Auersperg and colleagues have speculated that Müllerian metaplasia is coupled to ovarian neoplasia, and that OSE cells gain growth advantages by acquiring Müllerian-like phenotypes (Auersperg et al., 2001). These authors have speculated that Müllerian-like differentiation of OSE cells may increase responsiveness to hormones, because estrogen is mitogenic for Müllerian epithelium but not for normal OSE. Increased homophilic cell adhesion might also prevent anoikis. Unlike Müllerian epithelium, normal OSE has only a tenuous attachment to underlying stromal components, and therefore Müllerian-like differentiation of OSE cells may enhance epithelial–stromal interactions (Auersperg et al., 2001). These explanations for the ‘gain’ of Müllerian-like differentiation by OSE cells are compelling, but have not been tested experimentally.

Patterning of the reproductive tract is tightly regulated by homeobox genes (Kobayashi and Behringer, 2003). Homeobox genes were first discovered in *Drosophila* by their mutations that caused homeotic transformation, a phenomenon in which body segments form in an inappropriate location or context (Gehring and Hiromi, 1986). The mammalian *HOXA9*, *HOXA10* and *HOXA11* genes are uniformly expressed along the axis of the Müllerian ducts prior to differentiation, but their expression becomes spatially restricted in the primordia of the fallopian tubes, uterus, and lower uterine segment, respectively (Taylor et al., 1997). We have reported that this Müllerian *HOX* gene program is not expressed in normal OSE, but is recapitulated in ovarian cancers according to the patterns of Müllerian-like differentiation of these tumors (Cheng et al., 2005). Moreover, differential activation of *HOX* genes in transformed OSE cells induced tumors with distinct types of Müllerian-like features. Transformed mouse OSE cells that expressed *Hoxa10* formed tumors that resembled high-grade endometrioid carcinoma, whereas those that expressed *Hoxa9* and *Hoxa11* formed serous-like and mucinous-like tumors, respectively (Cheng et al., 2005).

HOXA10 is the most characterized Müllerian *HOX* gene, and is essential for controlling uterine patterning (Benson et al., 1996). *HOXA10* is expressed in ovarian cancers that have endometrial-like features (Cheng et al., 2005). In this study, we focused on *HOXA10* as a prototype Müllerian lineage-determining gene to test the hypothesis of Auersperg and colleagues that OSE cells gain a growth advantage by acquiring a Müllerian phenotype. Our findings indicate that activation of *HOXA10* in OSE cells prevents anoikis and enhances epithelial-stromal interactions that promote cell growth. These findings indicate that activation of a Müllerian program in OSE cells confers growth advantages in part by stimulating interactions with the microenvironment.

2. Materials and Methods

2.1. Reagents

Fibronectin, vitronectin, collagen I, laminin, and β-estradiol were purchased from Sigma (St. Louis, MO). The following antibodies (Abs) were used for Western blot and cell staining: HOXA10 (Aviva Systems Biology, San Diego, CA); αv integrin (clone AV1, Millipore, Temecula, CA); β3 integrin (clone B3A, Millipore); β1 integrin (clone MAR4, BD Biosciences, San Jose, CA); E-cadherin (Zymed, San Francisco, CA); actin (Sigma-Aldrich). The following Abs were used for cell staining and blocking: αvβ3 integrin (clone LM609, Millipore); α2β1 integrin (clone BHA2.1, Millipore). Secondary Abs were as follows: horseradish peroxidase-

conjugated Abs (BioRad, Hercules, CA); Alexa Fluor-conjugated Abs (Invitrogen, Carlsbad, CA); PerCP-conjugated Abs (BD Biosciences).

2.2. Cell transfection

The human OSE cell line T29 (Liu et al., 2004) was provided by Jinsong Liu (M.D. Anderson Cancer Center, Houston), and cultured in a 1:1 mixture of MCDB 105 medium (Sigma-Aldrich) and Medium 199 (Invitrogen) supplemented with 10% fetal bovine serum, epidermal growth factor (10 ng/ml) and penicillin-streptomycin. To generate T29-GFP cells that stably express green fluorescent protein (GFP), the *GFP* cDNA was subcloned into pLPCX vector (BD Biosciences) and the retroviral construct was used to transfect Ampho-293 cells (provided by Douglas Boyd, M.D. Anderson Cancer Center). Supernatants were harvested two days thereafter and used to infect T29 cells. T29-GFP cells were transfected using FuGENE6 (Roche, Indianapolis, IN) with human *HOXA10* cDNA (provided by Corey Largman, Veterans Affairs Medical Center, San Francisco) that was subcloned into pcDNA4 vector (Invitrogen). Control lines were generated by transfecting T29-GFP cells with empty pcDNA4 vector. Stably transfected clones, derived from single colonies, were selected by zeocin (200 μg/ml). The transformed mouse OSE cell line (MOSEC) which stably expresses mouse *Hoxa10* is described in our previous work (Cheng et al., 2005). The Ishikawa endometrial cancer cell line was provided by Russell Broaddus (M.D. Anderson Cancer Center).

2.3. Western blot and immunofluorescence staining

Cell lysates were prepared by using MPER buffer (Pierce Biotechnology, Rockford, IL), separated by SDS-PAGE and transferred to PVDF membranes (GE Healthcare USA, Piscataway, NJ). For detection of staining by immunofluorescence microscopy, cells were plated in chamber slides, fixed in 4% paraformaldehyde and permeabilized for 15 min in 0.1% Triton X-100. Cells were incubated for 1 h at 4°C with integrin Abs or E-cadherin Ab (1:100), washed and incubated with Alexa Fluor 594-conjugated secondary Ab. For detection of staining by flow cytometry, cells were harvested, incubated with integrin Abs (10 μg/ml) for 45 min at 4°C, washed and incubated with PerCP-conjugated secondary Ab. Following washing, cells were fixed in 4% paraformaldehyde and staining analyzed by flow cytometry (FACS Calibur, BD Biosciences).

2.4. Reverse-transcription (RT)-PCR

Reverse transcription using 1 μg of DNase I-treated total RNA was performed using Superscript II reverse transcriptase (Invitrogen) in a reaction volume of 20 μl. One microliter of RT reaction was used for amplification using Platinum Taq DNA polymerase (Invitrogen). Primers were as follows: β3 integrin: sense, 5′-GTCATCCCTGGCCTCAAGTC-3′; antisense, 5′-TGTTGCAGCGATGGCTATTA-3′; αv integrin: sense, 5′-ATGAAACAGGAGCGAGAGCC-3′; antisense, 5′-CGACAGCCACAGAATAACCC-3′; actin: sense, 5′- ATGATATCGCCGCGCTCG-3′; antisense, 5′-CGCTCGGTGAGGATCTTCA-3′. Amplification was performed as follows: denaturation at 95°C for 30 sec, annealing at 55°C for 30 sec, extension at 72°C for 30 sec for 33 cycles (for β3 integrin); denaturation at 95°C for 30 sec, annealing at 59°C for 30 sec, extension at 72°C for 30 sec for 30 cycles (for αv integrin); denaturation at 95°C for 30 sec, annealing at 55°C for 30 sec, extension at 72°C for 30 sec for 28 cycles (for actin). Titrations were performed to ensure a linear range of amplification.

2.5. Proliferation and anoikis assays

For proliferation assays, 2,000 cells were seeded per well in 96-well plates. Proliferation was measured by using the 3-(4,5-dimethylthiazolyl-2)-2,5-diphenyltetrazolium bromide (MTT) assay (Roche). To prevent cell attachment, 12-well plates were coated with poly(2-

hydroxyethyl methacrylate) (polyHEMA)(Sigma) (10 mg/ml in 95% ethanol) and dried overnight. One hundred thousand cells were seeded per well. After three days, aliquots of cells were removed from each well for staining with trypan blue dye and counting using a hemocytometer. A total of 5×10^4 cells from each well was harvested, and mono- and oligo-nucleosomes were detected in cell lysates by using the cell death detection ELISA (Roche). All assays were performed in triplicate in two independent experiments.

2.6. Adhesion assays

Primary cultures of normal mesothelial cells and fibroblasts were isolated from omental tissues of patients undergoing surgery for benign conditions as previously described (Kenny et al., 2007). Omental fibroblasts (15,000) and mesothelial cells (30,000) were seeded in 96-well plates to generate confluent monolayers. Wells were also precoated with fibronectin, vitronectin, collagen I and laminin (0.5 μg per well). After one day, 15,000 T29-GFP cells were seeded per well. For blocking experiments, T29-GFP cells were pre-incubated for 30 min with integrin Abs or mouse IgG at a final concentration of 10 μg/ml, and then seeded on to fibroblast and mesothelial cell monolayers. After incubation at 37°C for the indicated times, cells were washed 5 times in phosphate-buffered saline to remove unattached cells. Cells were fixed in 4% paraformaldehyde and viewed by immunofluorescence microscopy using a fluorescein filter. Attached T29-GFP cells were counted in three random fields of 0.2 mm^2 in each of three replicate wells. Adhesion assays were performed in triplicate in two independent experiments.

2.7. Co-culture assays

For direct co-culture assays, omental fibroblasts (1,000) were seeded with 1,000 T29-GFP cells per well in 96-well plates. After culture for the indicated times, cells were fixed in 4% paraformaldehyde, stained with 4′,6-diamidino-2-phenylindole (DAPI), and viewed by immunofluorescence microscopy. T29-GFP cells (GFP+, DAPI+) and fibroblasts (GFP−, DAPI+) were counted in three random fields of 0.2 mm^2 in each of three replicate wells. For indirect co-culture assays, fibroblasts (2,000) and T29-GFP cells (2,000) were separately seeded in the upper and lower chambers, respectively, of 24-well transwell co-culture plates (BD Biosciences). Assays were performed in triplicate in two independent experiments.

2.8. Propagation of cells in mice

Ten 4-week-old female nude mice were inoculated i.p. with 10^6 cells of each MOSEC cell line. After 3 months, mice were sacrificed by CO_2 asphyxiation. Pelvic peritoneal tissues were excised, mounted on a black surface and photographed under a Leica MZML III microscope. For each mouse, the numbers of peritoneal implants were counted in five random fields of 1.0 cm^2. Sections of paraffin-embedded tissues were stained with HOXA10 Ab as previously described (Cheng et al., 2005).

2.9. Statistical analysis

Statistical significance of differences in the number of peritoneal implants in mice was calculated by Mann-Whitney *U*-test. Statistical significance of differences in cell proliferation, apoptosis and adhesion between vector-control and +HOXA10 cells was calculated by Student *t*-test. *P* values >0.05 were considered not significant.

3. Results

3.1. *HOXA10* prevents anoikis but does not increase responsiveness to estrogen

Because primary cultures of OSE cells only survive for a few passages, we used the T29 cell line as a model for our study. The T29 line is non-tumorigenic, and derives from normal human

OSE cells that were immortalized by SV40 T antigens and *hTERT* (Liu et al., 2004). We isolated clones of T29 cells from single colonies that stably expressed *HOXA10* and clones transfected with empty vector [Fig.1A]. We first investigated whether *HOXA10* promotes cell proliferation. As shown in Fig.1B, growth rates of +HOXA10 T29 clones were not different from growth rates of vector-control clones. We also determined whether *HOXA10* increases responsiveness of T29 cells to β-estradiol. Whereas Ishikawa endometrial cancer cells proliferated in response to β-estradiol, vector-control and +HOXA10 T29 clones were equally unresponsiveness to β-estradiol [Fig.1C].

We next sought to determine whether *HOXA10* prevents anoikis by culturing T29 clones in plates coated with polyHEMA, an inert polymer that prevents cells from attaching to surfaces of plates. When cultured in polyHEMA-coated wells, +HOXA10 T29 clones formed larger aggregates than vector-control clones [Fig.1D]. Similar results were obtained using stable lines generated from MOSEC cells [Fig.1D]. MOSEC cells derive from mouse OSE cells that have spontaneously transformed in culture (Roby et al., 2000). The increased aggregation of +HOXA10 OSE cells did not appear to be associated with enhanced cell proliferation, as there was no net increase in the total numbers of cells following culture in polyHEMA-coated wells [Fig.1E]. However, the proportion of viable cells, as determined by the exclusion of trypan blue dye, was higher in cultures of +HOXA10 cells than in cultures of vector-control cells [Fig. 1E]. To confirm that HOXA10 prevents apoptosis under anchorage-inhibited conditions, mono- and oligo- nucleosome generation was assayed in equivalent numbers of T29 and MOSEC cells after culture in polyHEMA-coated and uncoated plates. Both vector-control and +HOXA10 clones underwent cell death when cell anchorage was inhibited by polyHEMA [Fig.1F]. However, cell death was significantly reduced in +HOXA10 clones, as compared to vector-control clones [Fig.1F]. Consistent with the increased aggregation of +HOXA10 cells, increased levels of Ecadherin were detected in +HOXA10 cells, particularly on the cell surface [Fig.1G]. Together, these findings indicate that induction of *HOXA10* confers a growth advantage to OSE cells by enhancing homophilic cell adhesion and preventing anoikis, but not by increasing responsiveness to estrogen.

3.2. *HOXA10* promotes adhesion to mesothelial cells

Ovarian cancer typically spreads via the transport of exfoliated tumor cells by the flow of peritoneal fluid. These cells commonly implant onto the mesothelial lining of the pelvic cavity (peritoneum), bowel serosa and the omentum (Naora and Montell, 2005; Kenny et al., 2007). The omentum is a fold of tissue comprised of fibroblasts and mesothelial cells that is suspended over the intestines. We sought to determine whether induction of *HOXA10* in OSE cells promotes adhesion of these cells to omental mesothelial cells. We stably expressed GFP in vector-control and +HOXA10 T29 lines to distinguish these cells from mesothelial cells. Adhesion assays were performed by seeding equivalent numbers of vector-control and +HOXA10 T29-GFP cells onto confluent monolayers of omental mesothelial cells. As shown in Fig.2A, the number of +HOXA10 T29-GFP cells that bound to omental mesothelial cells was significantly greater than the number of bound vector-control T29-GFP cells. We also determined whether expression of *HOXA10* in tumorigenic OSE cells promotes attachment to mesothelial surfaces *in vivo*. For this purpose, we used the MOSEC cell line. When propagated i.p. in nude mice, vector-control MOSEC cells form solid, undifferentiated tumors, whereas MOSEC cells that stably express *Hoxa10* form glandular-like tumor nests (Cheng et al., 2005) [Fig.2B]. We found that mice inoculated with +HOXA10 MOSEC cells developed a greater number of peritoneal implants than mice inoculated with an equivalent number of vector-control MOSEC cells [Fig.2C].

3.3. *HOXA10* promotes OSE cell interactions with extracellular matrix (ECM) proteins

The attachment of ovarian cancer cells to mesothelial surfaces is mediated in part by interactions between various ECM proteins and their receptors (Casey and Skubitz, 2000; Heyman et al., 2008). Adhesion assays were performed by seeding equivalent numbers of vector-control and +HOXA10 T29-GFP cells onto plates coated with different ECM proteins. As shown in Fig.3A, the number of +HOXA10 cells that bound to fibronectin and to vitronectin were significantly greater than the number of bound vector-control cells. Staining of the αvβ3 integrin heterodimer which binds both vitronectin and fibronectin (Reddy and Mangale, 2003) was more strongly detected in +HOXA10 cells than in vector-control cells [Fig.3B]. As compared to vector-control cells, +HOXA10 cells were more strongly inhibited from binding to omental mesothelial cells by Ab to αvβ3 integrin (52% *vs.* 83% inhibition) [Fig.3C]. Consistent with these observations, increased expression of the αv and β3 integrin subunits was detected at the mRNA [Fig.3D] and protein [Fig.3E] levels in +HOXA10 cells, as compared to vector-control cells (2.5-fold and 1.6-fold increase for αv and β3 proteins respectively, as determined from mean fluorescence intensities).

HOXA10 was less effective in stimulating cell adhesion to type I collagen and laminin than to vitronectin and fibronectin [Fig.3A]. Consistent with this observation, we found little difference in expression of α2β1 integrin, which preferentially binds collagen and laminin (Casey and Skubitz, 2000;Reddy and Mangale, 2003), in vector-control and +HOXA10 cells [Fig.3B]. Vector-control and +HOXA10 cells were similarly inhibited by α2β1 Ab from binding to mesothelial cells (41% *vs*. 47% inhibition) [Fig.3C]. It has been previously found that induction of *HOXA10* in endometrial cells does not alter expression of β1 integrin (Yoshida et al., 2006). We likewise observed no difference in β1 integrin levels in vector-control and +HOXA10 OSE cells [Fig.3E].

3.4. *HOXA10* enhances interactions with fibroblasts that promote OSE cell growth

In subsequent experiments, we investigated whether induction of *HOXA10* in OSE cells enhances interactions with omental fibroblasts. Equivalent numbers of vector-control and +HOXA10 T29-GFP cells were seeded onto confluent monolayers of omental fibroblasts. The number of +HOXA10 T29-GFP cells that bound to omental fibroblasts was significantly greater than that of vector-control T29-GFP cells [Fig.4A]. As compared to vector-control cells, +HOXA10 cells were more strongly inhibited by Ab to v 3 integrin from binding to fibroblasts (68% *vs.* 84% inhibition). On the other hand, vector-control and +HOXA10 cells were equally inhibited by Ab from binding to fibroblasts (49% *vs*. 50% inhibition) [Fig.4B].

Because fibroblasts play an important role in supporting growth of epithelial cells, we investigated whether *HOXA10* promotes growth of OSE cells when these cells are cultured in direct contact with fibroblasts. Growth rates of +HOXA10 T29-GFP clones were significantly faster than growth rates of vector-control clones when co-cultured in direct contact with omental fibroblasts [Figs.4C,D]. However, the growth rates of +HOXA10 clones were not different from growth rates of vector-control clones in the absence of fibroblasts [compare Fig. 4D with Fig.1B]. In addition, growth rates of fibroblasts co-cultured with +HOXA10 T29-GFP cells were not significantly different from growth rates of fibroblasts co-cultured with vector-control T29-GFP cells [Fig.4E]. These findings indicate that induction of *HOXA10* in OSE cells promotes interactions with fibroblasts, and these enhanced direct cell-cell interactions confer a growth advantage to OSE cells.

We also investigated whether *HOXA10* promotes growth of OSE cells when these cells are cultured with fibroblasts but without direct contact. In contrast to our observations in direct co-culture assays [Fig.4D], the numbers of +HOXA10 T29-GFP cells were not significantly different from numbers of vector-control cells following co-culture with fibroblasts in transwell

plates for up to five days [Fig.4F]. However, numbers of +HOXA10 cells were higher than those of vector-control cells at the latest time point assayed (Day 7) [Fig.4F]. We therefore cannot entirely exclude the possibility that HOXA10 might also increase the responsiveness of OSE cells to paracrine factors released by fibroblasts.

4. Discussion

The debate questioning the OSE origin of ovarian cancers, and the search for an alternative Müllerian precursor, has been driven by a lack of explanation for the Müllerian-like features exhibited by many of these tumors. The tubal fimbria has been suggested as an origin for high-grade serous ovarian carcinomas (Lee et al., 2007). The origin of endometrioid ovarian carcinomas has also been subject to controversy. Endometriosis is associated with endometrioid carcinoma in 21 to 43% of cases (Ogawa et al., 2000; Sainz de la Cuesta et al., 1996). In one mouse genetic model, activation of K-*ras* in the OSE induced endometriotic-like lesions, and endometrioid-like tumors were induced by a combination of K-*ras* activation and *Pten* loss (Dinulescu et al., 2005). However, the link between endometriosis and endometrioid carcinoma suggested by this model has been questioned because *KRAS* mutations rarely occur in endometriosis (Wu et al., 2007). A more recent model demonstrated that inactivation of *Pten* and *Apc* in the OSE induces endometrioid-like tumors without associated endometriosis (Wu et al., 2007).

Auersperg *et al*. have alternatively speculated that the prevalence of Müllerian phenotypes in ovarian cancers reflects the primordial relationship between the OSE and Müllerian ducts, and confers selective growth advantages to OSE cells (Auersperg et al., 2001). This hypothesis resonates with an emerging model of carcinogenesis in which dominant phenotypic alterations are viewed as successful adaptive strategies used by a tumor to overcome microenvironmental selection pressures (Anderson et al., 2006; Gatenby and Gillies, 2008). Ovarian cancer cells need to adapt to two dynamic changes in their microenvironment. The first occurs when cells are exfoliated and transported by the flow of peritoneal fluid. The second occurs when cells implant onto mesothelial surfaces such as the peritoneum and omentum. Our study demonstrates that activation of *HOXA10*, a homeobox gene that controls Müllerian differentiation, promotes homophilic cell adhesion and prevents anoikis in OSE cells. Our study also demonstrates that induction of *HOXA10* enhances interactions of OSE cells with omental fibroblasts and that these epithelial-stromal interactions promote OSE cell growth. Phenotypic alterations induced by Müllerian ‘mis-programming’ in OSE-derived cells might represent an adaptive strategy that enables these cells to survive as floating cells and to colonize distal sites.

The endometrioid subtype of ovarian cancer histologically resembles its counterpart in the uterine corpus, but these tumors encounter profoundly different microenvironmental changes. One similarity between these two types of tumors is the control by *HOXA10* of glandular differentiation. We have reported that *HOXA10* expression is down-regulated in endometrial carcinomas and correlates with loss of glandular differentiation (Yoshida et al., 2006). On the other hand, gain of *HOXA10* expression correlates with glandular differentiation in endometrioid ovarian tumors (Cheng et al., 2005). Activation of *HOXA10* promotes homophilic cell adhesion in endometrial epithelial cells (Yoshida et al., 2006) and also in OSE cells. In both of these cell types, the increased homophilic cell adhesion induced by *HOXA10* appears to be attributed at least in part to increased E-cadherin expression. However, whereas *HOXA10* activation in endometrial cancer cells inhibits tumor dissemination (Yoshida et al., 2006), we observed that *HOXA10* activation in OSE-derived tumor cells lead to increased numbers of peritoneal implants. These paradoxical findings explain a fundamental difference between i.p. seeding of ovarian cancer, and the ’classic’ metastasis of endometrial cancer and most other types of carcinomas. ‘Classic’ metastasis involves invasion of surrounding tissues,

the crossing of vascular endothelium, and extravasation into surrounding tissue at a distant site (Fidler, 2003). Although ovarian cancer can initially spread by extending to adjacent organs, hematogenous dissemination is rare (Naora and Montell, 2005). Ovarian cancer typically spreads by i.p. seeding, whereby tumor cells are exfoliated and transported by the flow of peritoneal fluid and attach to mesothelial surfaces. It is likely that this mode of dissemination is promoted when OSE-derived cells are able to escape anoikis, and when the ability of these cells to adhere to and grow on mesothelial surfaces, is increased.

Adhesion of ovarian cancer cells to mesothelium is mediated by interactions of various integrins such as αvβ3, α2β1 and α6β1, and by integrin-independent mechanisms such as CD44-hyaluronan interactions (Casey and Skubitz, 2000; Heyman et al., 2008). Our study indicates that *HOXA10* promotes interactions of OSE cells with mesothelial surfaces at least in part by increasing expression levels of αvβ3 integrin, though other mechanisms cannot be excluded. The finding that *HOXA10* induces αvβ3 integrin expression is consistent with the observation of increased levels of αvβ3 in differentiated ovarian cancers (Carreiras et al., 1996) and the ability of *HOXA10* to induce tumor differentiation (Cheng et al., 2005). Of note is that female mice with a targeted disruption of *Hoxa10* are unable to support embryo implantation (Benson et al., 1996). αvβ3 integrin is important for implantation, and levels of *HOXA10* and αvβ3 integrin in the endometrium increase during the window of receptivity (Reddy and Mangale, 2003; Sarno et al., 2005). Indeed, the *ITGB3* gene that encodes β3 integrin has been reported to be a transcriptional target of HOXA10 in endometrial and myeloid cells (Daftary et al., 2002; Bei et al., 2007). In this study, we found that activation of *HOXA10* in OSE cells induces expression of β3 and also αv integrin. Further study is required to determine whether the genes encoding αv and β3 integrins are direct transcriptional targets of HOXA10 in OSE cells. Another goal for future study is the identification of the mechanisms that activate *HOX* genes in ovarian cancers. Possible mechanisms might involve deregulation by Polycomb group proteins and by sex steroid signaling. Because *HOX* genes appear to function downstream of sex steroids (Ma et al., 1998), it is not surprising that *HOXA10* did not alter the responsiveness of OSE cells to β-estradiol.

In summary, our study demonstrates that the phenotypic alterations induced by Müllerian ‘mis-programming’ confer significant growth advantages to OSE cells. Our study raises the possibility that the dominance of Müllerian phenotypes in ovarian cancers might reflect an evolutionary strategy by these cancers to adapt to dynamic changes in their microenvironment.

Acknowledgments

This work was supported by NIH grant R01 CA101826 (to H.N.). We thank Pamela Ghosh, Nicolas Barengo and Wenjun Cheng (M.D. Anderson Cancer Center) for assistance with cell transfection, plasmid preparation and xenograft generation, respectively, and Soguel Dogan (University of Chicago) for assistance with omental cell cultures.

Abbreviations

ECM	extracellular matrix
OSE	ovarian surface epithelium

References

Anderson AR, Weaver AM, Cummings PT, Quaranta V. Tumor morphology and phenotypic evolution driven by selective pressure from the microenvironment. Cell 2006;127:905–915. [PubMed: 17129778]

Auersperg N, Wong AS, Choi KC, Kang SK, Leung PC. Ovarian surface epithelium: biology, endocrinology, and pathology. Endocr. Rev 2001;22:255–288. [PubMed: 11294827]

Bei L, Lu Y, Bellis SL, Zhou W, Horvath E, Eklund EA. Identification of a HoxA10 activation domain necessary for transcription of the gene encoding beta3 integrin during myeloid differentiation. J. Biol. Chem 2007;282:16846–16859. [PubMed: 17439948]

Benson GV, Lim H, Paria BC, Satokata I, Dey SK, Maas RL. Mechanisms of reduced fertility in Hoxa-10 mutant mice: uterine homeosis and loss of maternal Hoxa-10 expression. Development 1996;122:2687–2696. [PubMed: 8787743]

Carreiras F, Denoux Y, Staedel C, Lehmann M, Sichel F, Gauduchon P. Expression and localization of alpha v integrins and their ligand vitronectin in normal ovarian epithelium and in ovarian carcinoma. Gynecol. Oncol 1996;62:260–267. [PubMed: 8751559]

Casey RC, Skubitz AP. CD44 and beta1 integrins mediate ovarian carcinoma cell migration toward extracellular matrix proteins. Clin. Exp. Metastasis 2000;18:67–75. [PubMed: 11206841]

Cheng W, Liu J, Yoshida H, Rosen D, Naora H. Lineage infidelity of epithelial ovarian cancers is controlled by HOX genes that specify regional identity in the reproductive tract. Nat. Med 2005;11:531–537. [PubMed: 15821746]

Connolly DC, Bao R, Nikitin AY, Stephens KC, Poole TW, Hua X, Harris SS, Vanderhyden BC, Hamilton TC. Female mice chimeric for expression of the simian virus 40 TAg under control of the MISIIR promoter develop epithelial ovarian cancer. Cancer Res 2003;63:1389–1397. [PubMed: 12649204]

Daftary GS, Troy PJ, Bagot CN, Young SL, Taylor HS. Direct regulation of 3-integrin subunit gene expression by HOXA10 in endometrial cells. Mol. Endocrinol 2002;16:571–579. [PubMed: 11875117]

Dinulescu DM, Ince TA, Quade BJ, Shafer SA, Crowley D, Jacks T. Role of Kras and Pten in the development of mouse models of endometriosis and endometrioid ovarian cancer. Nat. Med 2005;11:63–70. [PubMed: 15619626]

Dubeau L. The cell of origin of ovarian epithelial tumors. Lancet Oncol 2008;9:1191–1197. [PubMed: 19038766]

Feeley KM, Wells M. Precursor lesions of ovarian epithelial malignancy. Histopathology 2001;38:87–95. [PubMed: 11207821]

Fidler IJ. The pathogenesis of cancer metastasis: the ‘seed and soil’ hypothesis revisited. Nat. Rev. Cancer 2003;3:453–458. [PubMed: 12778135]

Flesken-Nikitin A, Choi KC, Eng JP, Shmidt EN, Nikitin AY. Induction of carcinogenesis by concurrent inactivation of *p53* and *Rb1* in the mouse ovarian surface epithelium. Cancer Res 2003;63:3459–3463. [PubMed: 12839925]

Gatenby RA, Gillies RJ. A microenvironmental model of carcinogenesis. Nat. Rev. Cancer 2008;8:56–61. [PubMed: 18059462]

Gehring WJ, Hiromi Y. Homeotic genes and the homeobox. Annu. Rev. Genet 1986;20:147–173. [PubMed: 2880555]

Guioli S, Sekido R, Lovell-Badge R. The origin of the Müllerian duct in chick and mouse. Dev. Biol 2007;302:389–398. [PubMed: 17070514]

Heyman L, Kellouche S, Fernandes J, Dutoit S, Poulain L, Carreiras F. Vitronectin and its receptors partly mediate adhesion of ovarian cancer cells to peritoneal mesothelium in vitro. Tumor Biol 2008;29:231–244.

Kenny HA, Krausz T, Yamada SD, Lengyel E. Use of a novel 3D culture model to elucidate the role of mesothelial cells, fibroblasts and extracellular matrices on adhesion and invasion of ovarian cancer cells to the omentum. Int. J. Cancer 2007;121:1463–1472. [PubMed: 17546601]

Kobayashi A, Behringer RR. Developmental genetics of the female reproductive tract in mammals. Nat. Rev. Genet 2003;4:969–980. [PubMed: 14631357]

Lee Y, Miron A, Drapkin R, Nucci MR, Medeiros F, Saleemuddin A, Garber J, Birch C, Mou H, Gordon RW, Cramer DW, McKeon FD, Crum CP. A candidate precursor to serous carcinoma that originates in the distal fallopian tube. J. Pathol 2007;211:26–35. [PubMed: 17117391]

Liu J, Yang G, Thompson-Lanza JA, Glassman A, Hayes K, Patterson A, Marquez RT, Auersperg N, Yu Y, Hahn WC, Mills GB, Bast RC Jr. A genetically defined model for human ovarian cancer. Cancer Res 2004;64:1655–1663. [PubMed: 14996724]

Ma L, Benson GV, Lim H, Dey SK, Maas RL. Abdominal B (AbdB) Hoxa genes: regulation in adult uterus by estrogen and progesterone and repression in Müllerian duct by the synthetic estrogen diethylstilbestrol (DES). Dev. Biol 1998;197:141–154. [PubMed: 9630742]

Naora H, Montell DJ. Ovarian cancer metastasis: Integrating insights from disparate model organisms. Nat. Rev. Cancer 2005;5:355–366. [PubMed: 15864277]

Naora H. The heterogeneity of epithelial ovarian cancers: reconciling old and new paradigms. Expert Rev. Mol. Med 2007;9:1–12. [PubMed: 17477890]

Ogawa S, Kaku T, Amada S, Kobayashi H, Hirakawa T, Ariyoshi K, Kamura T, Nakano H. Ovarian endometriosis associated with ovarian carcinoma: a clinicopathological and immunohistochemical study. Gynecol. Oncol 2000;77:298–304. [PubMed: 10785482]

Orsulic S, Li Y, Soslow RA, Vitale-Cross LA, Gutkind JS, Varmus HE. Induction of ovarian cancer by defined multiple genetic changes in a mouse model system. Cancer Cell 2002;1:53–62. [PubMed: 12086888]

Reddy KV, Mangale SS. Integrin receptors: the dynamic modulators of endometrial function. Tissue Cell 2003;35:260–273. [PubMed: 12921709]

Roby KF, Taylor CC, Sweetwood JP, Cheng Y, Pace JL, Tawfik O, Persons DL, Smith PG, Terranova PF. Development of a syngeneic mouse model for events related to ovarian cancer. Carcinogenesis 2000;21:585–591. [PubMed: 10753190]

Sainz de la Cuesta R, Eichhorn JH, Rice LW, Fuller AF Jr. Nikrui N, Goff BA. Histologic transformation of benign endometriosis to early epithelial ovarian cancer. Gynecol. Oncol 1996;60:238–244. [PubMed: 8631545]

Sarno JL, Kliman HJ, Taylor HS. HOXA10, Pbx2 and Meis1 protein expression in the human endometrium: formation of multimeric complexes on HOXA10 target genes. J. Clin. Endocrinol. Metab 2005;90:522–528. [PubMed: 15494461]

Taylor HS, Vanden Heuvel GB, Igarashi P. A conserved Hox axis in the mouse and human female reproductive system: late establishment and persistent adult expression of the Hoxa cluster genes. Biol. Reprod 1997;57:1338–1345. [PubMed: 9408238]

Wu R, Hendrix-Lucas N, Kuick R, Zhai Y, Schwartz DR, Akyol A, Hanash S, Misek DE, Katabuchi H, Williams BO, Fearon ER, Cho KR. Mouse model of human ovarian endometrioid adenocarcinoma based on somatic defects in the Wnt/beta-catenin and PI3K/Pten signaling pathways. Cancer Cell 2007;11:321–333. [PubMed: 17418409]

Yoshida H, Broaddus R, Cheng W, Xie S, Naora H. Deregulation of the HOXA10 homeobox gene in endometrial carcinoma: Role in epithelial-mesenchymal transition. Cancer Res 2006;66:889–897. [PubMed: 16424022]

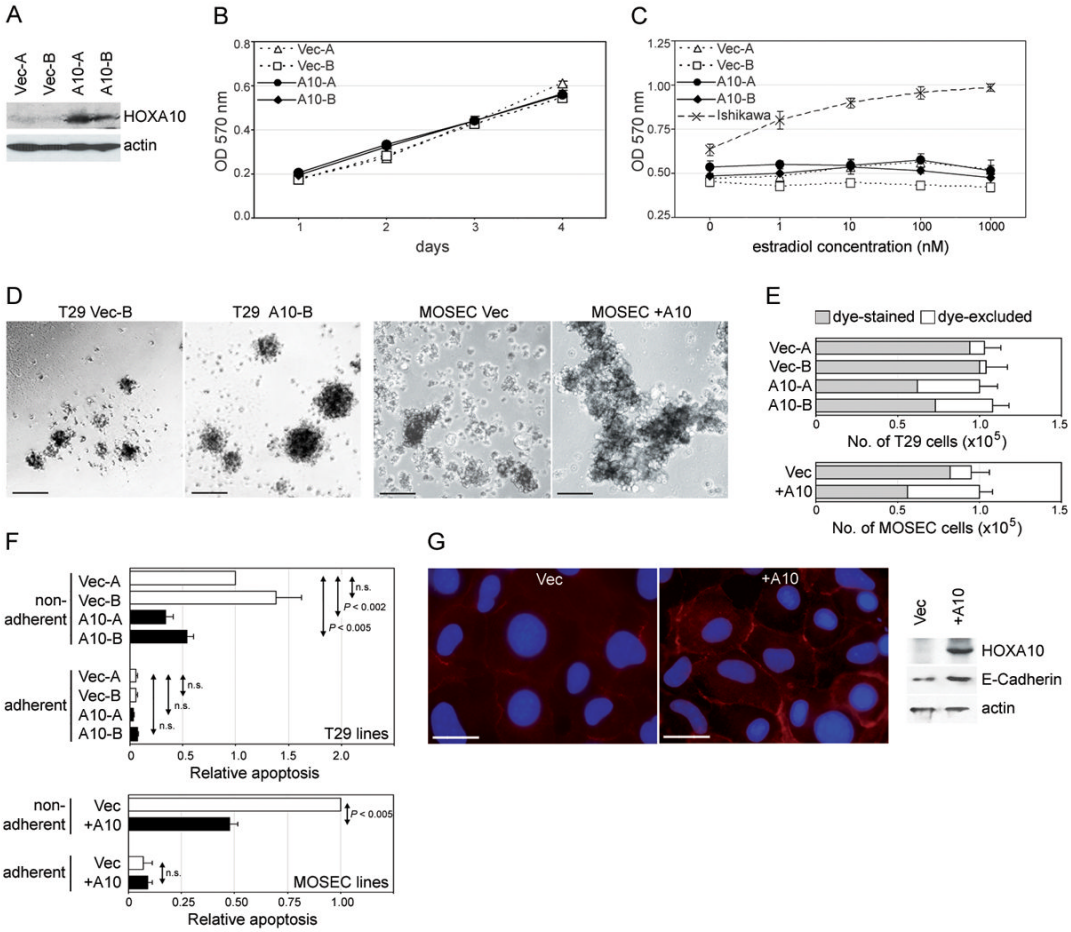

Fig.1. Effects of *HOXA10* on cell proliferation and anoikis

(A) Western blot of HOXA10 in vector-control (Vec-A, Vec-B) and +HOXA10 (A10-A, A10-B) T29 clones. (B) Growth of T29 clones cultured in uncoated plates was measured on the indicated days by MTT assay. (C) Growth of Ishikawa cells and T29 clones was measured by MTT assay at 3 days after addition of the indicated concentrations of β-estradiol. In (D-F), 100,000 cells of each vector-control and +HOXA10 T29 and MOSEC line were seeded in polyHEMA-coated wells and cultured for 3 days. In (D), cells were viewed under phase-contrast light microscopy. Bar, 100 μm. (E) Aliquots of cells from each well were stained with trypan blue dye and counted using a hemocytometer. Shown are the total numbers of cells per well and the proportions of viable cells (dye-excluded, shown in white) and non-viable cells (dye-stained, shown in grey). (F) Apoptosis was determined by assaying mono- and oligo-nucleosome generation in equivalent numbers of T29 and MOSEC cells (5×10^4) at 3 days after culture in polyHEMA-coated and uncoated plates. Levels of apoptosis are expressed relative to the levels of apoptosis detected in Vec-A cells (for T29 lines) and in Vec cells (for MOSEC lines) under non-adherent conditions. All assays were performed in triplicate in two independent experiments. (G) *Left*, immunofluorescence staining of MOSEC cells with E-cadherin Ab (red) and DAPI (blue). Bar, 20 μm. *Right*, E-cadherin expression detected by Western blot.

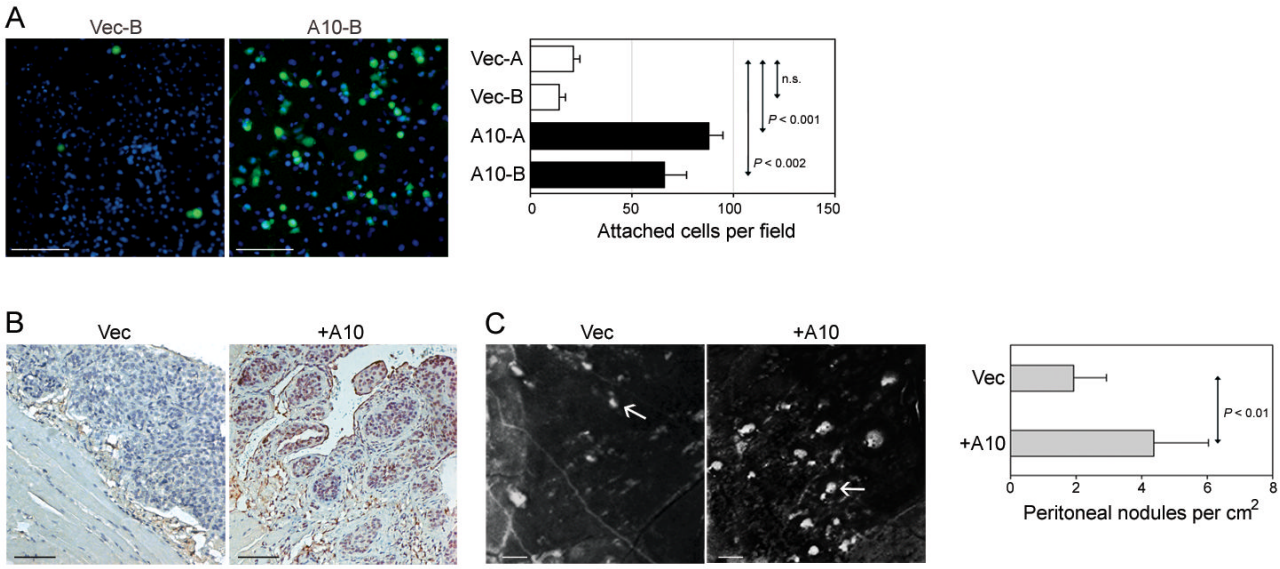

Fig.2. *HOXA10* promotes adhesion of OSE cells to mesothelial cells

(A) Equivalent numbers (15,000) of vector-control and +HOXA10 T29 cells that stably expressed GFP were seeded onto confluent monolayers of omental mesothelial cells. At 2 h thereafter, wells were washed, stained with DAPI and viewed by immunofluorescence microscopy. Bar, 100 μm. Shown are numbers of attached T29-GFP cells per 0.2 mm^2 field, where GFP+ cells were counted in three random fields in each of three replicate wells. Assays were performed in triplicate in two independent experiments. In (B,C), groups of female nude mice were inoculated i.p. at one site with equivalent numbers of cells (10^6) of vector-control and of +HOXA10 MOSEC lines, and sacrificed at 3 months thereafter. (B) Immunohistochemical staining of HOXA10 in peritoneal implants. Bar, 100 μm. (C) Peritoneal tissues were excised and photographed under a Leica MZML III microscope. Bar, 2 mm. For each mouse, numbers of peritoneal implants were counted in five random fields of 1.0 cm^2. Shown are average number of implants for each group of mice (n=10).

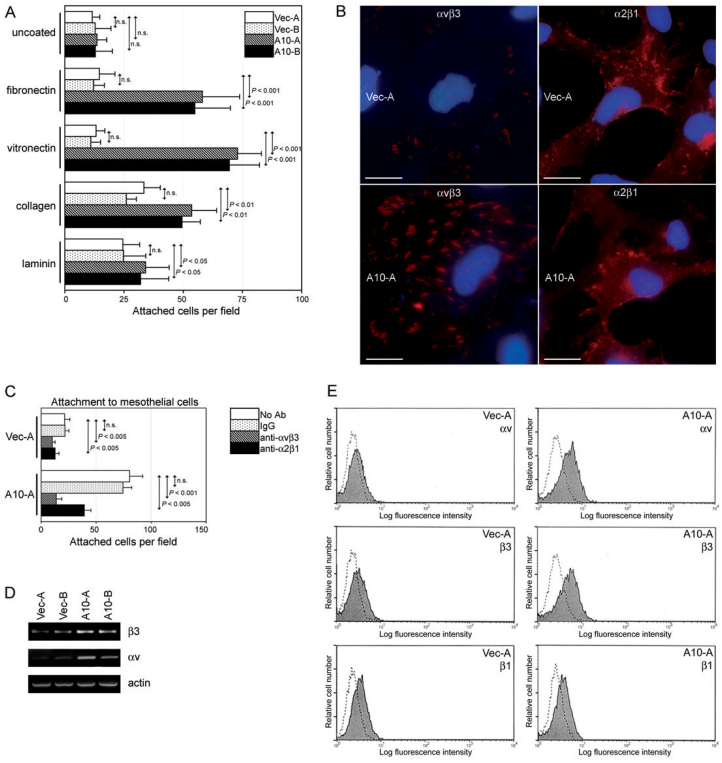

Fig.3. *HOXA10* promotes adhesion of OSE cells to ECM components

(A) Equivalent numbers (15,000) of vector-control and +HOXA10 T29-GFP cells were seeded onto wells coated with the indicated ECM proteins. At 1 h thereafter, attached T29-GFP cells counted in three random fields of 0.2 mm^2 in each of three replicate wells. (B) Immunofluorescence staining of αvβ3 and α2β1 integrins. Bar, 20 μm. (C) Equivalent numbers (15,000) of vector-control and +HOXA10 T29-GFP cells were pre-incubated with no Ab, mouse IgG, αvβ3 Ab, and α2β1 Ab, and seeded onto confluent monolayers of omental mesothelial cells. At 2 h thereafter, numbers of attached T29-GFP cells were counted as described in (A). Adhesion assays were performed in triplicate in two independent experiments. (D) Detection of transcripts of β3 and αv integrins in T29 clones by semi-quantitative RT-PCR. (E) Flow cytometric analysis of staining of β3, αv and β1 integrins (shaded regions), and negative control staining with secondary Ab alone (dotted lines) in T29 cells.

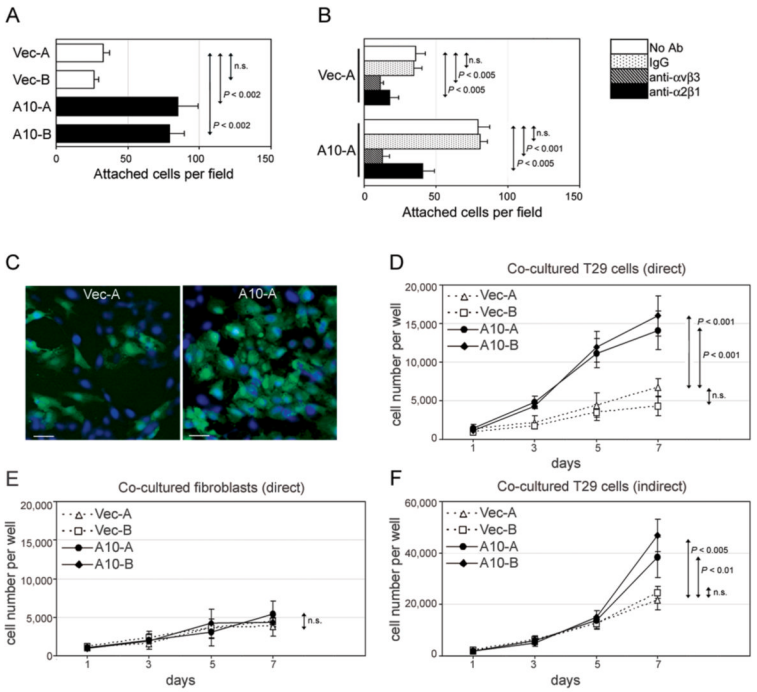

Fig.4. *HOXA10* promotes interactions of OSE cells with omental fibroblasts

(A) Equivalent numbers (15,000) of vector-control and +HOXA10 T29-GFP cells were seeded onto confluent monolayers of omental fibroblasts. At 2 h thereafter, attached T29-GFP cells were counted in three random fields of 0.2 mm^2 in each of three replicate wells. (B) Adhesion assays were likewise performed where T29-GFP cells were pre-incubated with no Ab, mouse IgG, αvβ3 Ab, and α2β1 Ab, and then seeded onto fibroblast monolayers. In (C-E), cells of each T29-GFP line (1,000) were seeded with 1,000 omental fibroblasts. After direct co-culture for the indicated times, cells were stained with DAPI and viewed by immunofluorescence microscopy. Shown in (C) are co-cultures of T29-GFP cells (GFP+, DAPI+) and fibroblasts (GFP−, DAPI+) on Day 5. Bar, 50 μm. Total numbers of (D) T29-GFP cells and (E) fibroblasts in each well were calculated based on cell counts in three random fields of 0.2 mm^2 in each of three replicate wells. In (F), 2,000 fibroblasts and 2,000 T29-GFP cells were seeded in the upper and lower chambers, respectively, of transwell co-culture plates. After indirect co-culture for the indicated times, the total number of T29-GFP cells in each well was determined by direct cell counts. All assays were performed in triplicate in two independent experiments.